Dendritic amphiphilic siRNA: Selective albumin binding, *in vivo* efficacy, and low toxicity

Hassan H. Fakih,[1,2] Qi Tang,[2] Ashley Summers,[2] Minwook Shin,[2,3] Julianna E. Buchwald,[2] Rosemary Gagnon,[2] Vignesh N. Hariharan,[2] Dimas Echeverria,[2] David A. Cooper,[2] Jonathan K. Watts,[2] Anastasia Khvorova,[2] and Hanadi F. Sleiman[1]

[1]Department of Chemistry, McGill University, Montreal, QC H3A 0B8, Canada; [2]RNA Therapeutics Institute, University of Massachusetts Chan Medical School, Worcester, MA 01605, USA; [3]College of Pharmacy, Sookmyung Women's University, Yongsan-gu, Seoul, Korea

Although an increasing number of small interfering RNA (siRNA) therapies are reaching the market, the challenge of efficient extra-hepatic delivery continues to limit their full therapeutic potential. Drug delivery vehicles and hydrophobic conjugates are being used to overcome the delivery bottleneck. Previously, we reported a novel dendritic conjugate that can be appended efficiently to oligonucleotides, allowing them to bind albumin with nanomolar affinity. Here, we explore the ability of this novel albumin-binding conjugate to improve the delivery of siRNA *in vivo*. We demonstrate that the conjugate binds albumin exclusively in circulation and extravasates to various organs, enabling effective gene silencing. Notably, we show that the conjugate achieves a balance between hydrophobicity and safety, as it significantly reduces the side effects associated with siRNA interactions with blood components, which are commonly observed in some hydrophobically conjugated siRNAs. In addition, it reduces siRNA monocyte uptake, which may lead to cytokine/inflammatory responses. This work showcases the potential of using this dendritic conjugate as a selective albumin binding handle for the effective and safe delivery of nucleic acid therapeutics. We envision that these properties may pave the way for new opportunities to overcome delivery hurdles of oligonucleotides in future applications.

INTRODUCTION

The interaction of therapeutic oligonucleotides with proteins in bodily fluids has a major influence on their pharmacokinetic and pharmacodynamic properties.[1,2] These interactions result in the adhesion of the proteins to oligonucleotides, thus altering the physical properties of the therapeutic modalities including their charge, size, shape, and surface chemistry. These properties can ultimately influence their biodistribution and therapeutic action *in vivo*.[3–5] This has been observed for simple chemical modifications to the sequence of oligonucleotides, such as phosphorothioate (PS)-modified backbones, as well as conjugates and nanoparticles (e.g., GalNAc, lipid nanoparticles) carrying these therapeutics.[1,3,6–9] In most cases, the binding of the oligonucleotides to serum proteins is not specific, which limits our understanding of each protein's role and influence.

The adhesion of biomolecules and proteins to the surface of therapeutics is not always correlated with negative outcomes.[8] Albumin, which accounts for 60% of total protein content in blood and interstitial tissues, represents an attractive protein target because of its ability to increase the half-life of therapeutics, improve pharmacokinetics, and aid their accumulation in solid tumors.[10] For example, albumin has been used in the U.S. Food and Drug Administration (FDA)-approved drug Abraxane, in which albumin-bound paclitaxel particles improve tumor delivery and efficacy compared with paclitaxel itself.[11] This is attributed to the albumin-increased localization in tumors via transcytosis-based transport, on the basis of albumin's receptor (gp60) and increased secretion of SPARC (secreted protein acidic and rich in cysteine) by tumors, a protein with high affinity to albumin.[12–14] Binding to albumin has been shown to improve the biodistribution of antisense oligonucleotides (ASOs), as it enables them to circulate to various organs such as interstitial tissues, liver, heart, lung, lymph nodes, and tumors.[10,11] Additionally, therapeutics have an increased half-life in circulation when albumin bound. This is a result of the non-degradative cellular uptake pathway via neonatal Fc receptor (FcRn) that rescues albumin from degradation in the lysosome and shuttles it back into circulation.[10,11,15] This has led to increased interest in the use of albumin for various applications, including nucleic acid therapeutics for tumor delivery, vaccine adjuvants, and improving extravasation to organs.[15–17]

However, careful design of albumin-binding ligands should be considered, as binding affinity and structure plays a pivotal role in cellular uptake and efficacy.[18] As albumin binds fatty acids, hydrophobic units need to be conjugated to oligonucleotides for albumin targeting. However, the precise design of these lipidic/hydrophobic

conjugates is essential, as they can also result in binding to other proteins in circulation.[19,20] Multiple studies have reported that changes in the design of conjugates intended to bind albumin, drastically impact their affinity and active delivery *in vitro*.[19,21] Hence, strong, selective, and carefully designed albumin-binding moieties are attractive modalities to append to nucleic acid therapeutics.[20]

We have previously developed a dendritic amphiphilic structure (Dendritic-1, abbreviated D in this study), that can be efficiently synthesized and appended to oligonucleotides in an automated fashion.[22] Despite its amphiphilic nature, the dendritic conjugate is completely soluble in an aqueous solution and does not aggregate or assemble into nanoparticles.[22] More interestingly, we showed that the conjugate by itself mediates exclusive albumin binding in serum with nanomolar affinity (K_d = 41 nM) *in vitro*, which was determined via surface plasmon resonance.[18] Such albumin-binding affinity and specificity reduce the probability of dynamic exchange between bound albumin and other serum proteins and encourage the exploration of its primary influence on the pharmacokinetics/dynamics of oligonucleotides.[23] We recently also performed a detailed cellular assessment on the impact of D-oligonucleotides, showing that they increase oligonucleotide stability, decrease non-specific cellular uptake and macrophage sequestering, and do not affect the silencing activity of the conjugated therapeutics in cells (both ASO and small interfering ribonucleic acid [siRNA]).[18,24] To explore the potential of D-oligonucleotides and the effect of binding albumin, *in vivo* experiments to assess their native interactions with proteins in circulation and to determine their biodistribution and their gene silencing activity are essential.

In this work, we investigate the properties and effect of the high-affinity albumin-binding dendritic conjugate D when attached to chemically stabilized siRNAs *in vivo*. We first assess the protein-binding profile *in vivo*, using size exclusion chromatography (SEC), by comparing dendritic-siRNA (D-siRNA) to an unconjugated siRNA (Unc-siRNA) and to a lipid-conjugated, lipoprotein-binding siRNA (docosanoic acid [DCA]; DCA-siRNA), which has previously shown potent gene activity *in vivo*.[9,25] We show that the D-siRNA selectively binds albumin, in comparison with DCA-siRNA, which binds predominantly to low-density lipoprotein (LDL)/high-density lipoprotein (HDL). Then, we study the biodistribution and silencing ability of D-siRNAs, and the data show promising efficacy in many organs (liver, heart, fat, injection site/back skin). Notably, the efficacy in the local injection site (dorsal skin) was particularly enhanced compared with the control DCA-siRNA conjugate tested. Gene silencing results for D-siRNA differ from the biodistribution/accumulation profile, measured using peptide nucleic acid (PNA) hybridization assay, and enhanced delivery is observed compared with DCA in the liver, kidney, distal skin, and adrenal glands. An initial toxicity screen via blood chemistry and complete blood count (CBC) at an increased dose showed no significant alterations compared with DCA, which shows a platelet decrease, indicating a better safety profile of the dendritic conjugate compared with more hydrophobic entities. Flow cytometry analysis following systemic injection shows that the dendritic conjugate reduces siRNA uptake into innate immune cells compared with the cholesterol conjugate. Hence, the work presented demonstrates the efficacy and safety of the dendritic moiety as an attractive conjugate for nucleic acid therapeutics, with selective albumin binding and a better safety profile.

RESULTS

D-siRNA has a favorable balance between hydrophobicity and hydrophilicity, with a selective protein-binding profile to albumin

We were interested in investigating the serum protein binding properties of D-siRNA, by performing a lipoprotein-binding profile study using SEC, as previously developed by Osborn et al.[9] The binding profile of a conjugate partly depends on its hydrophobicity, where more hydrophobic conjugates (e.g., docosanoic acid [DCA]) bind to LDL and LDL in plasma and to a lesser extent with albumin.[9] The dendritic moiety is larger and has more aliphatic material (69 carbons) compared with DCA (28 carbons). However, the multiple phosphates that punctuate the structure of the conjugate, in addition to the terminal hydroxyl group, lead to increased aqueous solubility and prevention of aggregation.[18,24] D-siRNA is less hydrophobic than DCA-siRNA, which is evident from lower retention when analyzed by reverse-phase high-performance liquid chromatography (RP-HPLC) (Figure 1A).

Following the hydrophobicity comparison by HPLC, we examined the serum protein-binding profile of each conjugate post-injection in mice as previously described.[9] Previously, we have demonstrated the ability of the dendritic moiety to bind albumin tightly and selectively *in vitro* when conjugated to oligonucleotides (Figure S2).[18,24] However, many hydrophobic conjugates will show albumin binding when measured in a test tube or *in vitro* that does not necessarily translate to *in vivo* binding.[9] Hence, we wanted to validate albumin binding from directly injected mice. Briefly, animals were injected either subcutaneously (s.c.) or intravenously (i.v.) with Cy3-labeled D-siRNA or DCA-siRNA at a dose of 10 mg/kg, and plasma was collected 15 min (for i.v.) and 60 min (for s.c.) post-injection. The time points were chosen to maximize the compounds circulating levels in the blood, as previously observed for those routes of administration.[26] Cy3 label for D-siRNA was placed between the 5′ end of the sense strand and the dendritic conjugate, to ensure no degradation or artifacts in the data.

The plasma was then fractionated using SEC and, the Cy3-siRNA elution time was monitored (at 570 nm). The elusion profile on a sucrose 6 size exclusion column for multiple major plasma proteins (HDL, very low density lipoprotein [VLDL], LDL, albumin/globulins) was previously established.[9] D-siRNA following injection into mice shows a sharp peak with a retention time at 67 min, which overlaps with that of albumin, compared with DCA-siRNA, which has a multi-protein-binding profile associated mostly with LDL and HDL (Figure 1B). The protein binding trend was consistent in both routes of administration. These data confirm the selective and high-affinity binding to albumin, which is hypothesized to dictate its behavior *in vivo* as it did *in vitro*.[18,24]
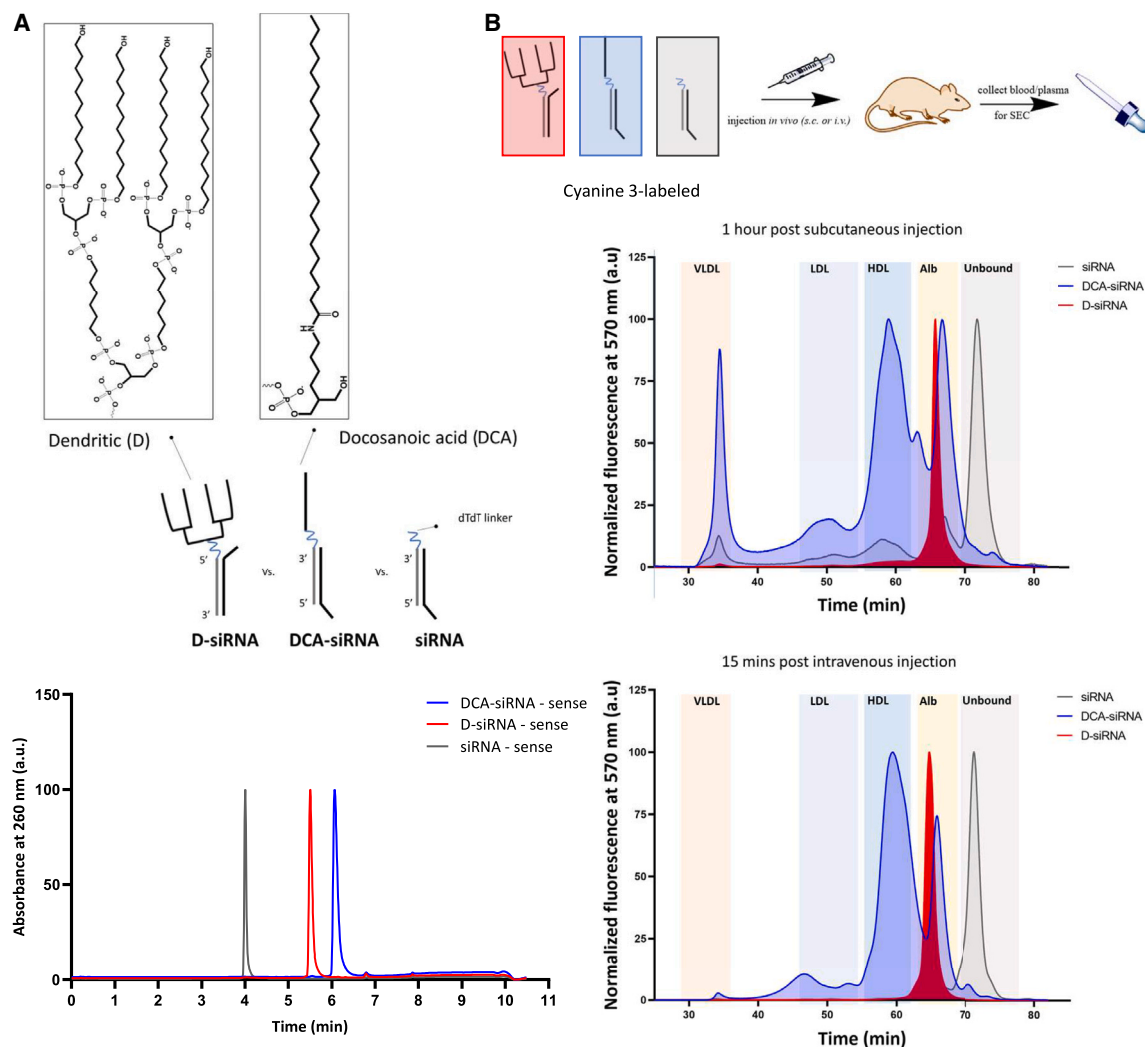
Figure 1. Physical properties of D-siRNAs
(A) Structure of the dendritic, docosanoic, and unconjugated siRNA tested for its hydrophobicity/retention time on high-performance liquid chromatography (HPLC), showing different retention times. (B) D-siRNA, DCA-siRNA, and siRNA were Cyanine-3 labeled and injected *in vivo* via subcutaneous or i.v. injection in mice (n = 2), and plasma was collected at 1 h or 15 min post-injection, respectively. Plasma was run on size exclusion chromatography (SEC), plasma proteins were monitored at 280 nm, and Cy3 labeled oligonucleotides were monitored at 570 nm, as previously reported. Elution signals were normalized to the highest peak.[9]

D-siRNA is active across multiple organs

To study the *in vivo* biodistribution and gene silencing efficacy of D-siRNA, we conjugated the dendritic moiety to fully chemically modified siRNAs targeting the ubiquitously expressed target Huntingtin (*Htt*).[27] We s.c. (dorsal skin) injected female mice with a single dose of 20 mg/kg non-targeting control (NTC)-DCA-siRNA, targeting positive control Htt-DCA-siRNA, or albumin-binding Htt-D-siRNA. Then, mRNA levels of *Htt* and *Hprt* (hypoxanthine-guanine phosphoribosyl transferase; a housekeeping gene) were measured 1 week post-injection in the major organs (Figure 2A). The data show significant silencing (compared with NTC) of the albumin-binding siRNA in the liver, dorsal skin (injection site), heart, adrenal glands, and fat.

We performed a previously reported PNA hybridization assay to quantify the Htt-antisense strand from the same experiment, to compare the silencing to biodistribution, as well as tissue retention (Figure 2B).[26] We found that D-siRNA distributes and retains in a range of organs at 1 week post-injection. Particularly, it a similar distribution profile as DCA-siRNA, showing accumulation in organs such as liver, heart, and lung. Interestingly, some organs' distribution did not always correlate with silencing efficacy. For example, D-siRNA was more active in gene silencing in the skin but accumulated to a much lesser extent, indicating that D-siRNA enters the blood stream faster and does not get stuck in the injection site. We also compared the distribution of siRNA, DCA-siRNA, and D-siRNA in major organs at 24 h post-injection and one week, showing the same distribution profile between time points,

A

B
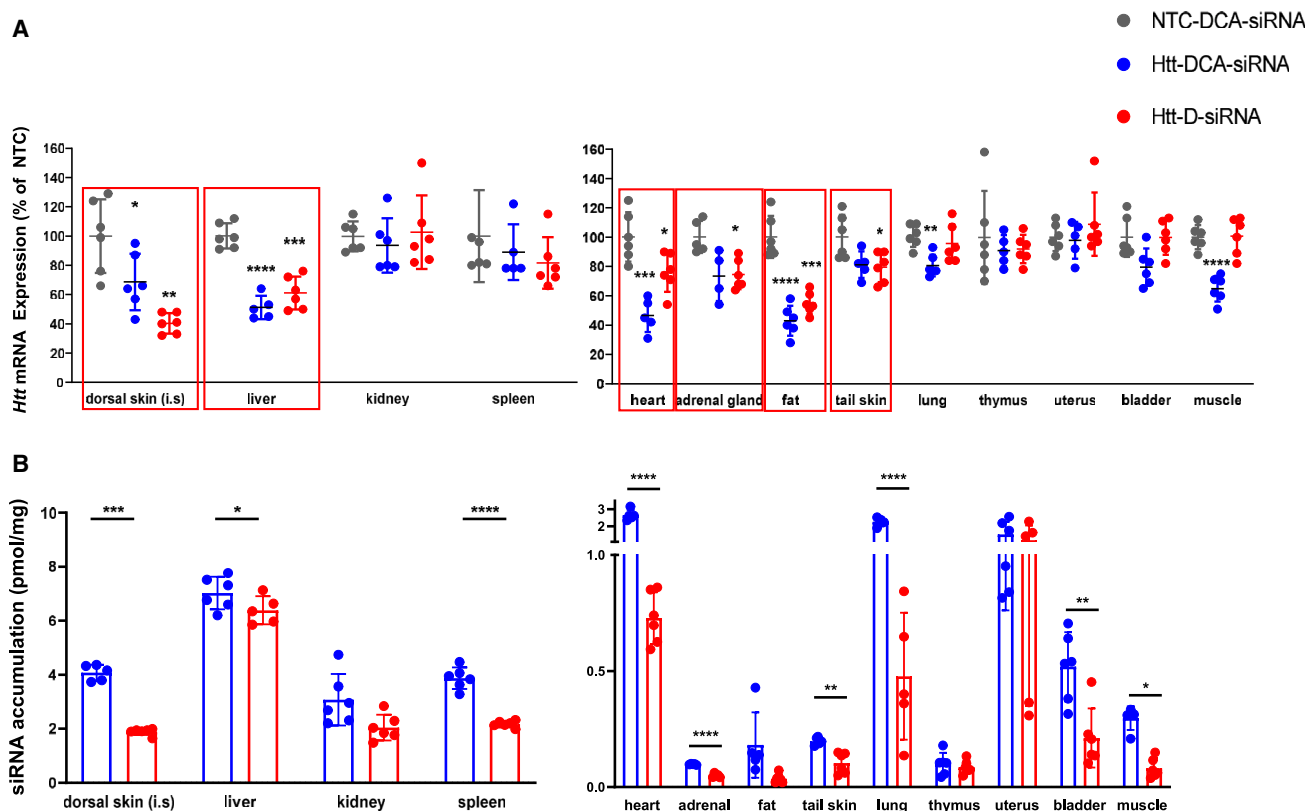
Figure 2. Measuring *in vivo* silencing activity of the dendritic conjugate, along with the standard DCA conjugate targeting *Htt* mRNA in mice

(A) Measurement of mRNA levels of Huntingtin gene in various organs using QuantiGene (Affymetrix), normalized to a housekeeping gene, Hprt (hypoxanthine-guanine phosphoribosyl transferase) and presented as percentage of NTC control (mean ± SD). (B) Bar graph showing accumulation of conjugate siRNA using PNA hybridization assay. mRNA levels and siRNA accumulation were from the same experiment, in which female mice (20 mg/kg; n = 5 or 6 mice per group ± SD) were injected a single subcutaneous injection of each compound and analyzed following 1 week. Data analysis: multiple comparisons, one-way ANOVA, Dunnett test (*p < 0.05, **p < 0.01, ***p < 0.001, and ****p < 0.0001). Distribution data analysis (B) is based on a t test.

with only a decrease in kidney accumulation for both conjugates between 24 h and one week post-injection (Figure S3).

Localization of D-siRNA in the tissues mentioned could be explained by the formation of albumin in the liver, and its increased circulation in interstitial tissues/spaces of the skin, muscle, lung, heart, kidneys, and spleen.[11,28,29] Apart from the liver, these organs have a continuous endothelium that expresses gp60 abundantly, which is the albumin-binding glycoprotein that could also explain the localization observed.[13] Albumin is also an ample component of lung lining fluids (concentration of about 10% of that found in serum)[30,31] This opens up the potential to harness the ability to hijack albumin's biodistribution to target these organs and spaces.[15]

D-siRNA shows a dose-dependent activity *in vivo*, validated against another target, CD47

We further confirmed the *in vivo* activity of D-siRNAs against a second target, *CD47*. *CD47* is another ubiquitously expressed protein which allows the examination of activity in various organs.[32,33] As some *Htt* mRNA can be located in the nucleus as previously re-

ported,[34] measuring *CD47* mRNA silencing might tease out subtle differences in activity between the studied conjugates. In this study, we also performed the experiment with a decreasing dose of the D-siRNA, ranging from 20 to 5 mg/kg. We observed a dose-dependent silencing of *CD47* mRNA with D-siRNA (Figure 3), to a similar extent observed in targeting *Htt* mRNA, confirming the decrease in mRNA is due to silencing.

D-siRNA has a better safety profile

We evaluated the general safety profile of D-siRNA *in vivo*. Mice were injected with an escalating dose of 100 mg/kg, the blood chemistry diagnostics and CBC were performed at 24 h. The data showed no detectable alteration of parameters in D-siRNA-injected mice compared with PBS-injected mice (Figure 4). However, an obvious platelet level decrease was observed with DCA-siRNA but not with D-siRNA, suggesting the dendritic conjugate may be a desirable moiety for improving the safety profile of therapeutic oligonucleotide.

Following this result, we further investigated whether D-siRNA may offer a better safety profile in reducing potential immune responses
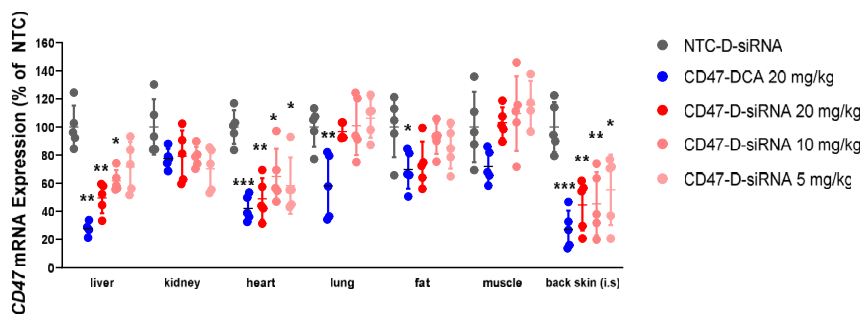
Figure 3. Dose-response activity *in vivo* of the dendritic conjugate targeting CD47 mRNA in mice

Measurement of mRNA levels of Huntingtin gene in various organs using QuantiGene (Affymetrix), normalized to a housekeeping gene, *Hprt* (hypoxanthine-guanine phosphoribosyl transferase) and presented as percentage of NTC control (mean ± SD). Female mice (20 mg/kg; n = 5 mice per group ± SD) were injected with a single subcutaneous injection of each compound/dose and analyzed following 1 week. Data analysis: multiple comparisons, one-way ANOVA, Dunnett test (*p < 0.05, **p < 0.01, ***p < 0.001, and ****p < 0.0001).

that are commonly associated with conjugated oligonucleotide therapeutics. Hydrophobic conjugates, such as cholesterol and DCA, stimulate the innate immune system as they are taken up by monocytes and leukocytes.[35–38] We previously reported that DCA- and cholesterol-conjugated siRNA have similar accumulation in bone marrow and uptake into immune cells, with DCA having slightly decreased uptake compared with cholesterol.[38]

Here, we performed a similar study, in which we examined the uptake of Cy3-labeled D-siRNA in the bone marrow and spleen, compared with cholesterol-siRNA using flow cytometry. Twenty-four hours after s.c. injection, the bone marrow and spleen of mice were collected and stained for lymphocytes and subtypes of leukocytes, to assess a broad profile of immune cell uptake. The gating strategy (Figure 5A) consists of first selecting singlet cells (forward scatter height [FSC-H] vs. forward scatter area [FSC-A]), followed by live immune cells (SYTOX Blue$^-$/CD45$^+$). Then, lymphocytes (CD11b$^-$) and leukocytes (CD11b$^+$) were segregated. Leukocytes were further dissected into sub-populations of neutrophils (CD11c$^-$, GR-1$^+$), eosinophils (CD11c$^-$, GR-1$^-$), and CD11c$^+$ monocytes. Dendritic cells (F40/80$^-$) and macrophages (F40/80$^+$) were gated from CD11c$^+$ cells in the spleen only (low count in bone marrow). Lymphocytes were segregated into T cells (CD19$^-$, CD3$^+$) and B cells (CD19$^+$, CD3$^-$). The fraction and intensity of Cy3-labeled siRNAs in each cell population were then analyzed using FlowJo software (Figures 5B and 5C).

D-siRNA shows a significantly decreased uptake into all types of immune cells in comparison with cholesterol-siRNAs, in both the spleen and bone marrow. Specifically, D-siRNA has a significantly decreased uptake in leukocytes of the spleen and bone marrow overall, as well as the macrophage sub-population in the spleen, which are responsible for cytokine response in the innate immune system. Decreased uptake of D-siRNA into macrophages was also visualized using microscopy of macrophages treated with siRNAs *in vitro* for 24 h (Figure S4). This supports the notion that the amphiphilic dendritic conjugate is an effective and safer alternative to other more hydrophobic conjugates (e.g., DCA and cholesterol).[38]

DISCUSSION

Harnessing the properties of albumin, such as long circulation half-life and transcytosis, is a promising strategy for nucleic acid therapeutics.[3,11,15] We have previously developed the dendritic conjugate,

which is a unique, amphiphilic chemical moiety that can be grown on a DNA synthesizer in an efficient, sequence-specific, and automated fashion. We demonstrated that it binds albumin in nanomolar affinity *in vitro*, while retaining full gene silencing activity when conjugated to ASOs or siRNAs. The binding affinity (K_d = 41 nM) of this dendritic conjugate outperforms most albumin-binding ligands reported in the literature (50 μM to 50 nM), including that of semaglutide (a drug developed by Novo Nordisk).[18,24,39]

In this work, we first confirmed that the dendritic conjugate binds albumin exclusively once injected *in vivo*, using an SEC-based protein binding experiment (Figure 1B). The data suggest that D-siRNA binds tightly to albumin and likely circulates as a protein-RNA complex in the blood until it extravasates into various organs and tissues. This observation appears to be independent of the routes of administration (i.e., s.c. or i.v.). A hydrophobic DCA conjugate, which has previously demonstrated potent silencing activity was used as a reference in this work. We demonstrate that the dendritic conjugate is more hydrophilic than DCA, which might be one of the properties to limit its interactions with HDL/LDL in plasma and to avoid undesired aggregation, a feature common to hydrophobic conjugates (e.g., cholesterol) (Figure 1A).[9] This might be attributed to the phosphates and hydroxyl groups present in the D-conjugate that increase its hydrophilicity, even if it is larger in size and has more aliphatic components than DCA (Figure 1A).[18] Thus, engineering therapeutic oligonucleotides with a balance between hydrophobicity and hydrophilicity might represent an important direction to improve their efficacy, distribution, and safety properties, as demonstrated in this work.

We assessed the silencing activity of D-siRNA by appending it to fully chemically modified siRNAs that target *Htt* mRNA, to assess body-wide activity. We compared the silencing activity of D-siRNAs with that of DCA-siRNAs, which have been shown to have silencing efficacy in a wide range of organs.[9,25,27] D-siRNAs showed efficient activity across multiple organs, especially in the liver, dorsal skin, adrenal glands, and fat (Figure 2A). This is the first *in vivo* silencing efficacy performed for this dendritic conjugate, demonstrating its efficient RNA-induced silencing complex (RISC) loading and gene silencing efficacy.[9,27] It is worth noting that the dendritic conjugate is placed on the 5′ end of the sense strand as it is grown via phosphoramidites in a sequential and automated fashion, and that the DCA conjugate is
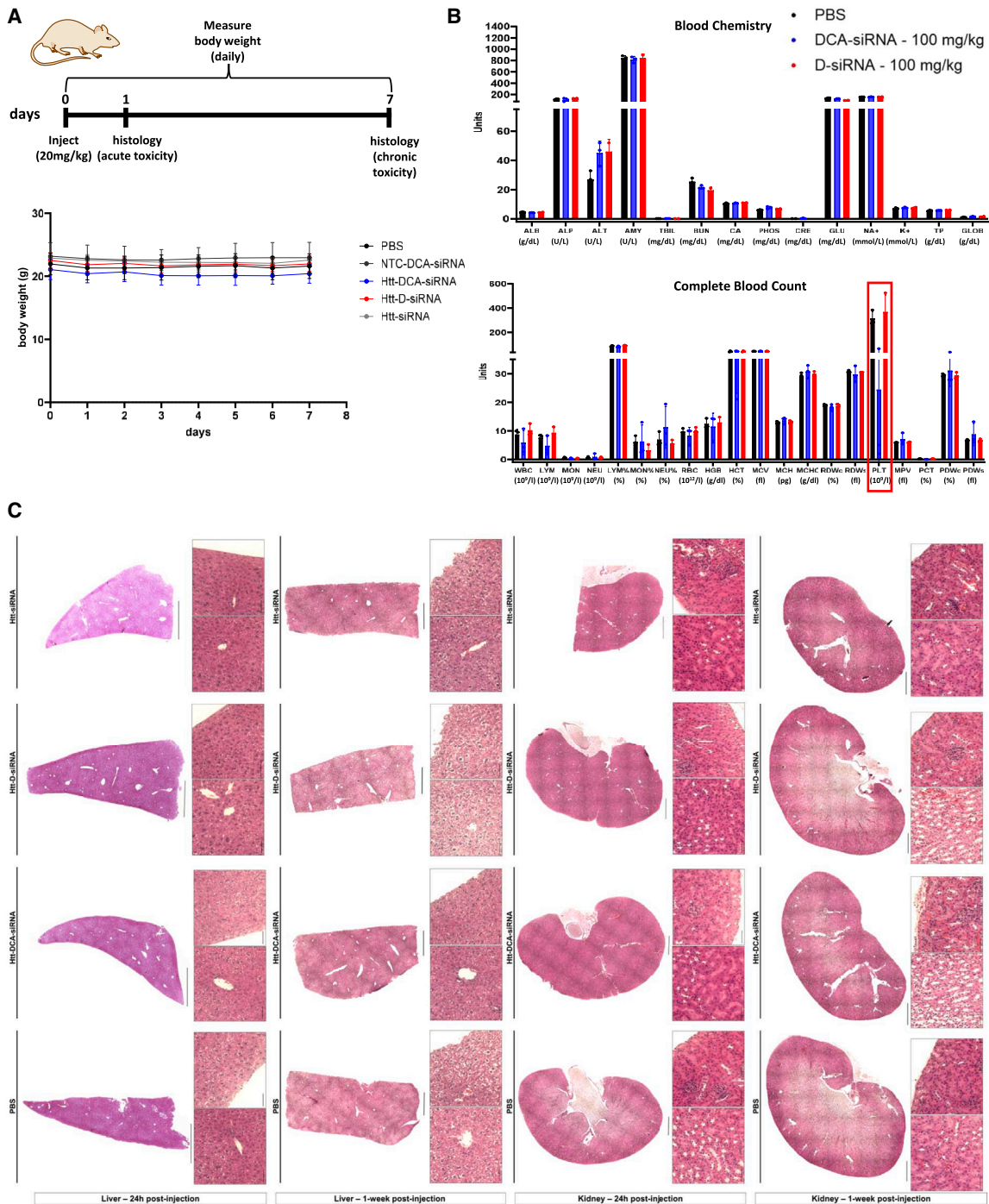
Figure 4. Safety of the dendritic conjugate

(A) Monitoring the body weight of mice injected with various siRNAs, demonstrating consistent body weight with no apparent changes. (B) Blood chemistry and complete blood count of mice (c56bl/6, male, n = 3) injected with DCA-siRNA or D-siRNA at 100 mg/kg, demonstrating a tolerated increased dose for D-siRNAs compared with DCA-siRNA that induces a platelet decrease. Blood was collected 24 h after subcutaneous injection. (C) Representative histology images of livers and kidneys that are H&E stained, showing no noticeable change or toxicity compared with control injected mice. Tile scans at 10× have a scale bar of 1 mm, and 40× images have a scale bar of 50 μm.
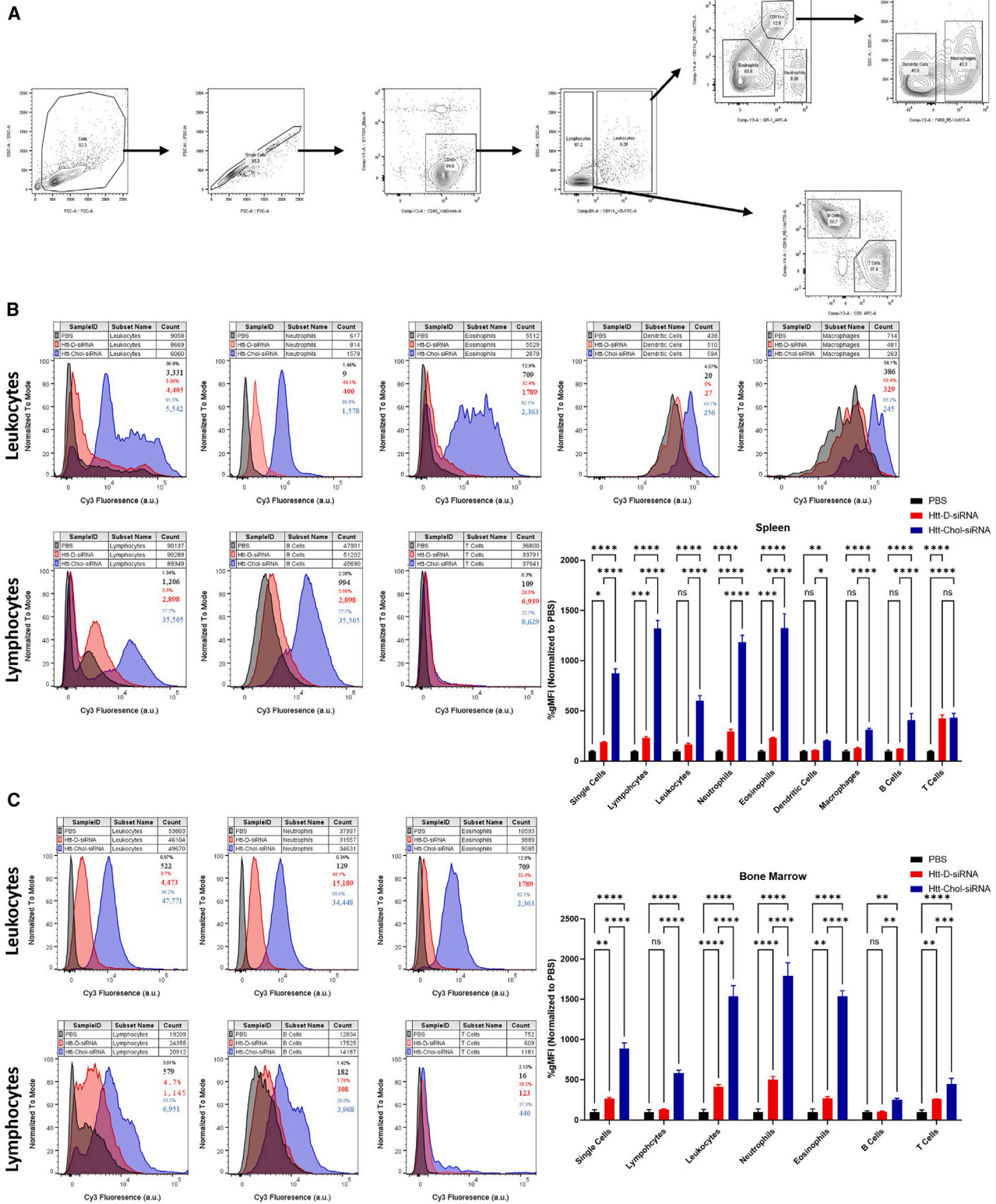
(legend on next page)

placed on the 3′ end of the sense strand as it is grown from a solid support.[18,27] We showed that the efficacy of siRNAs is identical whether the dendritic conjugate is placed on the 5′ or 3′ end, *in vitro* (Figure S1). This was done by synthesizing the D-siRNA using reverse amidites.

A PNA hybridization assay was performed to showcase the biodistribution of the Htt-siRNA. We found that D-siRNA distributed extra-hepatically to a number of organs, and was more present in the liver and kidney than DCA-siRNA while exhibiting similar activities (Figure 2B). Interestingly, it also showed a similar distribution in the local injection site (dorsal skin), but D-siRNA was significantly more active. This indicates that tissue accumulation and silencing efficacy do not always correlate, as has been previously reported.[27,40] Increased silencing in the dorsal skin or liver could be explained by increased cellular uptake into various cell types while having similar total organ accumulation. In other words, organ accumulation itself is not enough to produce efficacy, as non-degradative cellular uptake is still required in such organs. Albumin is known for its transcytosis uptake via gp60 and FcRn receptor, and endosomal/lysosomal escape following via the neonatal FcRn receptor that rescues it from that environment.[14,41] These receptors are expressed in many organs including liver, lung, and skin.[20] Hence, increased activity in the dorsal skin could be a result of a more effective cellular uptake of the D-siRNAs and localization into the cytoplasm for RISC loading.

As the dendritic conjugate has a lower hydrophobic profile, we were interested to assess its impact on the safety profile of interacting with blood components.[9,35] It is known that increased hydrophobicity of siRNA conjugates can cause side effects at higher doses, and lead to a cytokine and inflammatory response.[9,35,38] We assessed the impact of D-siRNA on blood chemistry and CBC at 24 h post-injection. At 100 mg/kg escalated dose, the dendritic conjugate showed no detectable alteration to the measured parameters, while DCA-siRNA caused a significant decrease in platelet count, which might be of a concern from safety perspective as it might cause thrombocytopenia. This suggests that the safety profile of D-siRNA is superior to certain hydrophobic conjugates due to its clean blood diagnostics at an escalated dose of 100 mg/kg (Figure 4).

Cytokine and inflammatory innate immune response are known to happen with certain hydrophobic conjugates such as cholesterol.[35–38] We previously reported that DCA and cholesterol-conjugated siRNA have similar accumulation in the bone marrow and uptake into immune cells, which is responsible for these inflammatory responses.[38] Even when DCA was modified with a positively charged molecule to improve its solubility (PC-DCA), it only slightly decreased the uptake into monocytes compared with cholesterol.[38] Here, we conducted a similar, but more comprehensive study to check whether the dendritic conjugate decreases immune cell uptake in both the bone marrow and the spleen, in comparison with cholesterol (Figure 5). Indeed, a large decrease in uptake into leukocytes and lymphocytes is observed with the D-siRNA in comparison with the immunostimulatory cholesterol-siRNA. The decrease is across multiple cell types, including neutrophils, dendritic cells, and macrophages (in the spleen). This further supports the safety profile and advantage of utilizing the dendritic conjugate, which supports desirable safe and efficient gene silencing properties.

In conclusion, we have tested, for the first time, the impact of albumin-binding dendritic moiety on the biodistribution and safety properties of therapeutic siRNAs *in vivo*. The data demonstrated that this dendritic conjugate supports selective binding to albumin following i.v. or s.c. injections. The biodistribution profile and activity of D-siRNA were assessed, showing a relatively broad distribution profile when injected systemically with significant gene silencing activity compared with the NTC. The broad distribution is a result of albumin binding, which improves circulation and reduces kidney clearance. Its activity was comparable with that of the previously studied DCA-siRNA compound, with better performance in some organs (adrenal, local injection site) at the time point studied (1 week). Additionally, it has an improved safety profile, with no detectable side effects from blood diagnostics, histology, or animal body weight. Moreover, the dendritic conjugate reduces siRNA accumulation in immune cells, which may lead to cytokine and inflammatory responses. This excellent safety profile of D-siRNAs comes from the albumin-binding ability, which enhances stability and decreases immune cell uptake, possibly by masking the negative charge of the oligonucleotide that can lead to uptake into immune cells via scavenger receptors.[42,43] The ease of manufacturing of these sequence-controlled conjugates with exclusive binding to albumin and effective silencing are attractive avenues for the field of therapeutic oligonucleotides, where applications for these properties are currently being pursued. Careful design and engineering of hydrophobic conjugates is an avenue worth exploring to control protein binding and further improve on efficacious delivery and safety.

MATERIALS AND METHODS

Oligonucleotide synthesis

Oligonucleotides were synthesized on a MerMade 6/12 synthesizer (BioAutomation) and AKTA Oligopilot 100 (GE Healthcare Life Sciences) following standard protocols. In brief, conjugated sense strands were synthesized at 5–20 μmol scales on custom-synthesized lipid-functionalized controlled pore glass (CPG) supports for DCA conjugate.[9,25,27] For the dendritic sense strand, synthesis was on CPG functionalized with UnyLinker (ChemGenes) and commercially available

Figure 5. Investigating immune cell uptake of D-siRNA

Flow cytometry analysis of spleen and bone marrow cells of mice (n = 3) 24 h post-injection subcutaneously with Cy3-labeled Htt-D-siRNA or Chol-D-siRNA. (A) Gating scheme in this experiment. (B and C) Frequency distribution histogram of Cy3 fluorescence intensity in different cells (left) and normalized geometric fluorescence intensity bar graph (right) in the (B) spleen and (C) bone. p values describe statistically significant differences relative to PBS control (2-way ANOVA, *p < 0.05, **p < 0.01, ***p < 0.001, and ****p < 0.0001). Percentage numbers in flow panels refer to percentage positive cells followed by the number of cells in the positive population.

Table 1. Oligonucleotide sequences synthesized and used in the project

Strands	Sequence (5′ to 3′)
D-sense (HTT targeting)	(C12)(SB)(C6)(SB)(dT)(dT)(mC)#(mA)#(mG)(mU)(fA)(fA)(fA)(mG)(fA)(mG)(mA)(mU)(mU)#(mA)#(mA)
DCA-sense (HTT targeting)	(mC)#(mA)#(mG)(mU)(fA)(fA)(fA)(mG)(fA)(mG)(mA)(mU)(mU)#(mA)#(mA)(dT)(dT)-DCA
Antisense (HTT targeting)	V(mU)#(fU)#(mA)(mA)(mU)(fC)(mU)(mC)(mU)(mU)(mU)(mA)(mC)#(fU)#(mG)#(fA)#(mU)#(mA)#(mU)#(fA)
DCA-NTC-sense (HTT experiment)	(mU)#(mG)#(mA)(mC)(fA)(fA)(fA)(mU)(fA)(mC)(mG)(mA)(mU)#(mU)#(mA)(dT)(dT)-DCA
NTC-antisense (HTT experiment)	V(mU)#(fA)#(mA)(mU)(mC)(fG)(mU)(mA)(mU)(mU)(mU)(mG)(mU)#(fC)#(mA)#(fA)#(mU)#(mC)#(mA)#(fU)
D-sense (CD47 targeting)	(C12)(SB)(C6)(S)(dT)(dT)(mU)#(mC)#(mA)(fC)(mA)(fU)(mA)(fA)(mA)(fU)(mG)(mA)(mU)(fU)#(mA)#(mA)
DCA-sense (CD47 targeting)	(mU)#(mC)#(mA)(fC)(mA)(fU)(mA)(fA)(mA)(fU)(mG)(mA)(mU)(fU)#(mA)#(mA) (dT)(dT)-DCA
Antisense (CD47 targeting)	V(mU)#(fU)#(mA)(fA)(fU)(fC)(mA)(fU)(mU)(fU)(mA)(fU)(mG)(fU)#(mG)#(fA)#(mC)#(mU)#(mU)#(fU)#(mU)
D-NTC-sense (CD47 experiment)	(C12)(SB)(C6)(S)(dT)(dT)(mA)#(mU)#(mU)(fG)(mA)(fC)(mA)(fA)(mA)(fU)(mA)(mC)(mG)(fA)#(mU)#(mA)
NTC-antisense (CD47 experiment)	V(mU)#(fA)#(mU)(fC)(fG)(fU)(mA)(fU)(mU)(fU)(mG)(mC)(fA)#(mA)#(fU)#(mC)#(mU)#(mU)#(fU)#(mU)
D-sense (protein binding experiment)	(C12)(SB)(C6)(S)(dT)(dT)(Cy3)#(mG)#(mU)#(mA)(fC)(mA)(fA)(mA)(fG)(mG)(fA)(mA)(mU)(mC)(fU)#(mG)#(mA)
DCA-sense (protein binding experiment)	(Cy3)#(mG)#(mU)#(mA)(fC)(mA)(fA)(mA)(fG)(mG)(fA)(mA)(mU)(mC)(fU)#(mG)#(mA)(dT)(dT)-DCA
Sense (protein binding experiment)	(Cy3)#(mG)#(mU)#(mA)(fC)(mA)(fA)(mA)(fG)(mG)(fA)(mA)(mU)(mC)(fU)#(mG)#(mA)(dT)(dT)
Antisense (protein binding experiment)	V(mU)#(fC)#(mA)(fG)(fA)(fU)(mU)(fC)(mC)(fU)(mU)(fU)(mG)(fU)#(mA)#(fC)#(mU)#(mU)#(mC)#(fA)#(mU)
Chol-sense (HTT targeting)	(mC)#(mA)#(mG)(mU)(fA)(fA)(fA)(mG)(fA)(mG)(mA)(mU)(mU)#(mA)#(mA)(dT)(dT)-Chol

#, PS backbone; m, 2′-o-methyl; f, 2′-fluoro; C12, hexaethylene spacer; C6, triethylene spacer; SB, symmetrical branching, I(E)-vinylphosphonate)

amidites (Cy3, C6, C12, and symmetrical branching from ChemGenes and Glen Research) were used to build the dendritic moiety on the 5′ end as previously described.[18,24] All sense strands had a 2dT spacer in between the strand and the conjugate. Antisense strands were synthesized on CPG functionalized with UnyLinker. They were first deprotected with a solution of bromotrimethylsilane/pyridine (3:2 v/v) in dichloromethane for the I-vinylphosphonate deprotection, then cleaved and deprotected with 28% aqueous ammonium hydroxide solution for 20 h at 60°C. All strands were cleaved and deprotected using 28% aqueous ammonium hydroxide solution for 20 h at 60°C, followed by drying under vacuum at 60°C, and resuspended in Millipore H_2O. Oligonucleotides were purified using an Agilent Prostar System (Agilent Technologies, Santa Clara, CA) over a C18 column for lipid-conjugated sense strands and over an ion-exchange column for antisense strands. Purified oligonucleotides were desalted by SEC and characterized by liquid chromatography-mass spectrometry (LC/MS) analysis on an Agilent 6530 accurate-mass quadrupole time-of-flight (Q-TOF) LC/MS (Agilent Technologies).

Sequences of the compounds and their modifications are in Table 1.

Injection of lipid-conjugated siRNAs into mice
Animal experiments of siRNA conjugates were performed in accordance with animal care ethics approval and guidelines of University of Massachusetts Medical School Institutional Animal Care and Use Committee (IACUC; protocol #202000010) at the RNA Therapeutics Institute. In all experiments, 7- to 8-week-old female FVB/NJ mice (The Jackson Laboratory) were used and were injected s.c. or i.v. with either NTC siRNA or lipid-conjugated siRNA (n = 5 or 6 per group) at a concentration of 20 mg/kg unless specified.

For distribution studies, 3 mice per sample were injected. For the efficacy studies, 5–8 mice per sample per gene were studied. For the toxicity studies, 3 mice per sample were injected.

In vivo mRNA silencing experiments
At 1 week post-injection, mice were euthanized and perfused with PBS. Tissues were collected and stored in RNAlater (Sigma-Aldrich) at 4°C overnight. mRNA was quantified using the QuantiGene (QG) 2.0 Assay (Affymetrix). The 1.5 mm punches (three punches per tissue) were placed in QIAGEN Collection Microtubes holding 3 mm tungsten beads and lysed in 300 μL Homogenizing Buffer (Affymetrix) containing 0.2 mg/mL Proteinase K (Invitrogen) using a QIAGEN TissueLyser II. Samples were then centrifuged at $1,000 \times g$ for 10 min and incubated for 1 h at 55°C to 60°C. Lysates and diluted probe sets (mouse *Htt*, mouse *Ppib*, or mouse *Hprt*) were added to the branched DNA (bDNA) capture plate, and signal was amplified and detected as described previously.[44] Luminescence was detected on a Tecan M1000 (Tecan, Morrisville, NC).

PNA hybridization assay
Tissue concentrations of antisense strands were determined using a PNA hybridization assay.[25,26] Tissues punches were placed in QIAGEN Collection Microtubes holding 3 mm tungsten beads and lysed in 300 μL MasterPure tissue lysis solution (EpiCentre) containing 0.2 mg/mL Proteinase K using a QIAGEN TissueLyser II. Lysates were then centrifuged at $1,000 \times g$ for 10 min and incubated for 1 h at 55°C to 60°C. Sodium dodecyl sulfate (SDS) was precipitated from lysates by adding 20 μL 3 M potassium chloride and pelleted centrifugation at $5,000 \times g$ for 15 min. Conjugated siRNAs in cleared supernatant were hybridized to a Cy3-labeled PNA probe fully

complementary to the antisense strand (PNABio, Thousand Oaks, CA). Samples were analyzed using HPLC (Agilent) over a DNAPac PA100 anion-exchange column (Thermo Fisher Scientific) in a gradient of sodium perchlorate, as follows: buffer A: 50% water, 50% acetonitrile, 25 mM Tris-HCl (pH 8.5), 1 mM ethylenediamine-tetraacetate; buffer B: 800 mM sodium perchlorate in buffer A. Gradient conditions were as follows: 10% buffer B within 4 min, 50% buffer B for 1 min, and 50%–100% buffer B within 5 min. Cy3 fluorescence was monitored and peaks integrated. Final concentrations were ascertained using calibration curves generated by spiking known quantities of lipid-conjugated siRNA into tissue lysates from an untreated animal. Spiked samples for calibration and experimental samples were processed and analyzed under the same laboratory conditions.

Microscopy
For histology, organs were collected from euthanized mice, washed with PBS, and fixed with formalin overnight. Then, organs were washed with PBS and provided to histology core for slicing and mounting using ProLong Gold Antifade Mountant with DAPI staining for nuclei. For *in vitro* fluorescent imaging, RAW 264.7 murine macrophages were grown in DMEM +10% FBS overnight in a 6-well coverslip dish., Cy3-labeled siRNA in 1xPBS were added to the cells for 24 h at 37°C, washed twice with PBS, DAPI stained, and imaged live. Data are available in the supplemental information.

Lipoprotein SEC
For lipoprotein profiling, we followed the same protocol previously described by Osborn et al.[9] Briefly, mice were injected i.v. with 10 mg/kg Cy3-labeled oligonucleotides. After 15 min, whole mouse blood (∼500 μL) was collected in a sterile ethylenediaminetetraacetic acid (EDTA)-coated tube following cheek incision with a lancet. Samples were spun at 10,000 rpm for 10 min at 4°C. Fifty microliters of plasma was directly injected on a Superose 6 Increase 10/300 size exclusion column (GE Healthcare). Oligonucleotide migration was monitored at 570 nm, and lipoprotein protein content was monitored by absorbance at 280 nm. For s.c. injections, we collected at 1 h post-injection.

Reverse-phase HPLC analysis of D-siRNA vs. DCA-siRNA
The LC data of oligonucleotides was performed on an Agilent 6530 accurate-mass Q-TOF using the following conditions: buffer A, 100 mM 1,1,1,3,3,3-hexafluoroisopropanol (HFIP) and 9 mM triethylamine (TEA) in LC/MS-grade water; buffer B, 100 mM HFIP and 9 mM TEA in LC/MS-grade methanol; column, Agilent AdvanceBio oligonucleotides C18; 5%–100% B 11 min; temperature, 60°C; flow rate, 0.5 mL/min. LC peaks were monitored at 260 nm.

Cell culture and *in vitro* dose response
HeLa cells were maintained in DMEM (10-013-CV; CellGro) supplemented with 10% fetal bovine serum (FBS) (26140; Gibco) and 100 U/mL penicillin/streptomycin (15140; Invitrogen) and expanded at 37°C and 5% CO_2. Seven-point dose-response curves were generated by treating HeLa cells with various concentrations of siRNA formu-

lated with RNAiMax (13778-150; Invitrogen) for 72 h at 37°C and 5% CO_2. Transfection was carried out in 50:50 DMEM/OptiMEM (31985-070; Gibco) and 3% FBS with no antibiotics. Cells were lysed by 30 min incubation at 55°C with diluted QG lysis mixture (QP0524; Invitrogen) containing Proteinase K. Gene silencing was assessed using QG bDNA assay per the manufacturer's instructions (see brief description below) using the following probe sets: mouse *Htt* (SB-14150) and mouse Hprt (SB-15463). *Htt* data were normalized to housekeeping *Hprt* and represented as the percentage of untreated control (n = 3).

Flow cytometry for immune cell uptake
Eight-week-old female mice were injected s.c. with a panel of Cy3-labeled siRNA variants. After 24 h, mouse femur bone was dissected, and femur bone marrow cells were isolated by flushing dissected femur bones with PBS using a 23G needle onto a 70 μm cell strainer placed in a 50 mL conical tube. The bone marrow and spleen were then smashed using a 5 mL plunger, followed by rinsing of the strainer with DMEM. The cell solution collected in the 50 mL tube was centrifuged at $350 \times g$ for 5 min at room temperature and washed once with PBS. Blood cells were lysed using ACK lysis buffer (155 mM NH_4Cl, 12 mM $NaHCO_3$, 0.1 mM EDTA in distilled water), followed by washing with DMEM ($500 \times g$, 10 min, 4°C). Next, the cell pellet was suspended with a flow cytometry buffer (0.5% BSA, 2 mM EDTA in DMEM) for flow cytometry analysis.

Leukocyte staining of the cell was with VioGreen-conjugated CD45 antibody (clone REA737; Miltenyi Biotec), allophycocyanin (APC)-conjugated GR-1 antibody (clone REA810; Miltenyi Biotec), fluorescein isothiocyanate (FITC)-conjugated CD11b antibody (clone REA592; Miltenyi Biotec), PE-Vio770-conjugated CD11c antibody (clone REA754; Miltenyi Biotec), and PE_Vio615 F40/80 (clone REA126; Miltenyi Biotec); for lymphocyte staining, PE-vio770 conjugated CD19 (clone REA749) and APC-conjugated CD3 antibody (clone REA641) were used. Cells were stained for 30 min at 4°C. Then, cells were washed twice with 700 μL flow cytometry buffer and resuspended in flow cytometry buffer containing 1 μM SYTOX Blue (Thermo Fisher Scientific). Stained cells were analyzed using a MACSQuant VYB Flow Cytometer (Miltenyi Biotec), and data were analyzed using FlowJo version 10.6 (BD Biosciences, Ashland, OR).

DATA AND CODE AVAILABILITY
All data presented in the main text and the supplemental information are available from the corresponding author upon request.

SUPPLEMENTAL INFORMATION
Supplemental information can be found online at https://doi.org/10.1016/j.omtn.2023.102080.

ACKNOWLEDGMENTS

AUTHOR CONTRIBUTIONS

H.H.F., A.K., and H.F.S. conceived and managed the project. H.H.F., D.A.C., and D.E. synthesized or helped with the synthesis of the siRNA compounds. H.H.F., Q.T., and A.S. conducted most *in vivo* experiments, and M.S., V.N.H., and J.K.W. helped with flow cytometry experimental design and execution. H.H.F., Q.T., and A.S. conducted the protein plasma-binding study. J.E.B. imaged all histology slides, and R.G. helped with siRNA tissue accumulation studies. H.H.F., A.K., and H.F.S. wrote the manuscript, with edits from Q.T. and M.S.

DECLARATION OF INTERESTS

H.H.F., A.K., and H.F.S. have filed a patent that covers the use of the dendritic conjugate *in vivo* for various applications. A.K. discloses ownership of stock in RXi Pharmaceuticals and Advirna; is a founder of Atalanta Therapeutics and Comanche Biopharma; and serves on the scientific advisory boards of Aldena Therapeutics, Prime Medicine, and Alltrna. V.N.H. is an employee of and holds stock options in Comanche Biopharma.

REFERENCES

1. Nguyen, V.H., and Lee, B.-J. (2017). Protein corona: a new approach for nanomedicine design. Int. J. Nanomed. *12*, 3137–3151.

2. Banker, M.J., and Clark, T.H. (2008). Plasma/serum protein binding determinations. Curr. Drug Metabol. *9*, 854–859.

3. Zhao, Z., Ukidve, A., Krishnan, V., and Mitragotri, S. (2019). Effect of physicochemical and surface properties on in vivo fate of drug nanocarriers. Adv. Drug Deliv. Rev. *143*, 3–21.

4. Albanese, A., Tang, P.S., and Chan, W.C.W. (2012). The Effect of Nanoparticle Size, Shape, and Surface Chemistry on Biological Systems. Annu. Rev. Biomed. Eng. *14*, 1–16.

5. de Castro, C.E., Panico, K., Stangherlin, L.M., Ribeiro, C.A.S., da Silva, M.C.C., Carneiro-Ramos, M.S., Dal-Bó, A.G., and Giacomelli, F.C. (2020). The Protein Corona Conundrum: Exploring the Advantages and Drawbacks of its Presence around Amphiphilic Nanoparticles. Bioconjugate Chem. *31*, 2638–2647.

6. Eckstein, F. (2014). Phosphorothioates, essential components of therapeutic oligonucleotides. Nucleic Acid Therapeut. *24*, 374–387.

7. Agarwal, S., Allard, R., Darcy, J., Chigas, S., Gu, Y., Nguyen, T., Bond, S., Chong, S., Wu, J.-T., and Janas, M.M. (2021). Impact of Serum Proteins on the Uptake and RNAi Activity of GalNAc-Conjugated siRNAs. Nucleic Acid Therapeut. *31*, 309–315.

8. Francia, V., Schiffelers, R.M., Cullis, P.R., and Witzigmann, D. (2020). The Biomolecular Corona of Lipid Nanoparticles for Gene Therapy. Bioconjugate Chem. *31*, 2046–2059.

9. Osborn, M.F., Coles, A.H., Biscans, A., Haraszti, R.A., Roux, L., Davis, S., Ly, S., Echeverria, D., Hassler, M.R., Godinho, B.M.D.C., et al. (2019). Hydrophobicity drives the systemic distribution of lipid-conjugated siRNAs via lipid transport pathways. Nucleic Acids Res. *47*, 1070–1081.

10. Kratz, F. (2008). Albumin as a drug carrier: design of prodrugs, drug conjugates and nanoparticles. J. Control Release. *132*, 171–183.

11. Hoogenboezem, E.N., and Duvall, C.L. (2018). Harnessing albumin as a carrier for cancer therapies. Adv. Drug Deliv. Rev. *130*, 73–89.

12. Andersen, J.T., and Sandlie, I. (2009). The versatile MHC class I-related FcRn protects IgG and albumin from degradation: implications for development of new diagnostics and therapeutics. Drug Metabol. Pharmacokinet. *24*, 318–332.

13. Schnitzer, J.E. (1992). gp60 is an albumin-binding glycoprotein expressed by continuous endothelium involved in albumin transcytosis. Am. J. Physiol. *262*, H246–H254.

14. Merlot, A.M., Kalinowski, D.S., and Richardson, D.R. (2014). Unraveling the mysteries of serum albumin-more than just a serum protein. Front. Physiol. *5*, 299.

15. Sarett, S.M., Werfel, T.A., Lee, L., Jackson, M.A., Kilchrist, K.V., Brantley-Sieders, D., and Duvall, C.L. (2017). Lipophilic siRNA targets albumin in situ and promotes bioavailability, tumor penetration, and carrier-free gene silencing. Proc. Natl. Acad. Sci. USA *114*, E6490–E6497.

16. Liu, H., Moynihan, K.D., Zheng, Y., Szeto, G.L., Li, A.V., Huang, B., Van Egeren, D.S., Park, C., and Irvine, D.J. (2014). Structure-based programming of lymph-node targeting in molecular vaccines. Nature *507*, 519–522.

17. Lau, S., Graham, B., Cao, N., Boyd, B.J., Pouton, C.W., and White, P.J. (2012). Enhanced Extravasation, Stability and in Vivo Cardiac Gene Silencing via in Situ siRNA–Albumin Conjugation. Mol. Pharm. *9*, 71–80.

18. Lacroix, A., Edwardson, T.G.W., Hancock, M.A., Dore, M.D., and Sleiman, H.F. (2017). Development of DNA Nanostructures for High-Affinity Binding to Human Serum Albumin. J. Am. Chem. Soc. *139*, 7355–7362.

19. Purdie, L., Alexander, C., Spain, S.G., and Magnusson, J.P. (2018). Alkyl-Modified Oligonucleotides as Intercalating Vehicles for Doxorubicin Uptake via Albumin Binding. Mol. Pharm. *15*, 437–446.

20. Bern, M., Sand, K.M.K., Nilsen, J., Sandlie, I., and Andersen, J.T. (2015). The role of albumin receptors in regulation of albumin homeostasis: Implications for drug delivery. J. Control Release. *211*, 144–162.

21. Felber, A.E., Bayó-Puxan, N., Deleavey, G.F., Castagner, B., Damha, M.J., and Leroux, J.-C. (2012). The interactions of amphiphilic antisense oligonucleotides with serum proteins and their effects on in vitro silencing activity. Biomaterials *33*, 5955–5965.

22. Edwardson, T.G.W., Carneiro, K.M.M., McLaughlin, C.K., Serpell, C.J., and Sleiman, H.F. (2013). Site-specific positioning of dendritic alkyl chains on DNA cages enables their geometry-dependent self-assembly. Nat. Chem. *5*, 868–875.

23. Monopoli, M.P., Åberg, C., Salvati, A., and Dawson, K.A. (2012). Biomolecular coronas provide the biological identity of nanosized materials. Nat. Nanotechnol. *7*, 779–786.

24. Lacroix, A., Fakih, H.H., and Sleiman, H.F. (2020). Detailed cellular assessment of albumin-bound oligonucleotides: Increased stability and lower non-specific cell uptake. J. Control Release. *324*, 34–46.

25. Biscans, A., Caiazzi, J., McHugh, N., Hariharan, V., Muhuri, M., and Khvorova, A. (2021). Docosanoic acid conjugation to siRNA enables functional and safe delivery to skeletal and cardiac muscles. Mol. Ther. *29*, 1382–1394.

26. Godinho, B.M.D.C., Gilbert, J.W., Haraszti, R.A., Coles, A.H., Biscans, A., Roux, L., Nikan, M., Echeverria, D., Hassler, M., and Khvorova, A. (2017). Pharmacokinetic Profiling of Conjugated Therapeutic Oligonucleotides: A High-Throughput Method Based Upon Serial Blood Microsampling Coupled to Peptide Nucleic Acid Hybridization Assay. Nucleic Acid Therapeut. *27*, 323–334.

27. Biscans, A., Coles, A., Haraszti, R., Echeverria, D., Hassler, M., Osborn, M., and Khvorova, A. (2019). Diverse lipid conjugates for functional extra-hepatic siRNA delivery in vivo. Nucleic Acids Res. *47*, 1082–1096.

28. Sand, K.M.K., Bern, M., Nilsen, J., Noordzij, H.T., Sandlie, I., and Andersen, J.T. (2014). Unraveling the Interaction between FcRn and Albumin: Opportunities for Design of Albumin-Based Therapeutics. Front. Immunol. *5*, 682.

29. Lomis, N., Sarfaraz, Z.K., Alruwaih, A., Westfall, S., Shum-Tim, D., and Prakash, S. (2021). Albumin Nanoparticle Formulation for Heart-Targeted Drug Delivery: In Vivo Assessment of Congestive Heart Failure. Pharmaceuticals 14, 697.

30. John, T.A., Vogel, S.M., Minshall, R.D., Ridge, K., Tiruppathi, C., and Malik, A.B. (2001). Evidence for the role of alveolar epithelial gp60 in active transalveolar albumin transport in the rat lung. J. Physiol. 533, 547–559.

31. Woods, A., Patel, A., Spina, D., Riffo-Vasquez, Y., Babin-Morgan, A., de Rosales, R.T.M., Sunassee, K., Clark, S., Collins, H., Bruce, K., et al. (2015). In vivo biocompatibility, clearance, and biodistribution of albumin vehicles for pulmonary drug delivery. J. Contr. Release 210, 1–9.

32. Dheilly, E., Moine, V., Broyer, L., Salgado-Pires, S., Johnson, Z., Papaioannou, A., Cons, L., Calloud, S., Majocchi, S., Nelson, R., et al. (2017). Selective Blockade of the Ubiquitous Checkpoint Receptor CD47 Is Enabled by Dual-Targeting Bispecific Antibodies. Mol. Ther. 25, 523–533.

33. Shin, M., Chan, I.L., Cao, Y., Gruntman, A.M., Lee, J., Sousa, J., Rodríguez, T.C., Echeverria, D., Devi, G., Debacker, A.J., et al. (2022). Intratracheally administered LNA gapmer antisense oligonucleotides induce robust gene silencing in mouse lung fibroblasts. Nucleic Acids Res. 50, 8418–8430.

34. Didiot, M.C., Ferguson, C.M., Ly, S., Coles, A.H., Smith, A.O., Bicknell, A.A., Hall, L.M., Sapp, E., Echeverria, D., Pai, A.A., et al. (2018). Nuclear Localization of Huntingtin mRNA Is Specific to Cells of Neuronal Origin. Cell Rep. 24, 2553–2560.e5.

35. Biscans, A., Coles, A., Haraszti, R., Echeverria, D., Hassler, M., Osborn, M., and Khvorova, A. (2019). Diverse lipid conjugates for functional extra-hepatic siRNA delivery in vivo. Nucleic Acids Res. 47, 1082–1096.

36. Nikan, M., Osborn, M.F., Coles, A.H., Godinho, B.M., Hall, L.M., Haraszti, R.A., Hassler, M.R., Echeverria, D., Aronin, N., and Khvorova, A. (2016). Docosahexaenoic acid conjugation enhances distribution and safety of siRNA upon local administration in mouse brain. Mol. Ther. Nucleic Acids 5, e344.

37. Alterman, J.F., Hall, L.M., Coles, A.H., Hassler, M.R., Didiot, M.-C., Chase, K., Abraham, J., Sottosanti, E., Johnson, E., Sapp, E., et al. (2015). Hydrophobically modified siRNAs silence huntingtin mRNA in primary neurons and mouse brain. Mol. Ther. Nucleic Acids 4, e266.

38. Davis, S.M., Hariharan, V.N., Lo, A., Turanov, A.A., Echeverria, D., Sousa, J., McHugh, N., Biscans, A., Alterman, J.F., Karumanchi, S.A., et al. (2022). Chemical optimization of siRNA for safe and efficient silencing of placental sFLT1. Mol. Ther. Nucleic Acids 29, 135–149.

39. Zorzi, A., Linciano, S., and Angelini, A. (2019). Non-covalent albumin-binding ligands for extending the circulating half-life of small biotherapeutics. Medchemcomm 10, 1068–1081.

40. Ly, S., Echeverria, D., Sousa, J., and Khvorova, A. (2020). Single-Stranded Phosphorothioated Regions Enhance Cellular Uptake of Cholesterol-Conjugated siRNA but Not Silencing Efficacy. Mol. Ther. Nucleic Acids 21, 991–1005.

41. Malhotra, A., and Mittal, B.R. (2014). SiRNA gene therapy using albumin as a carrier. Pharmacogenetics Genom. 24, 582–587.

42. Bijsterbosch, M.K., Manoharan, M., Rump, E.T., De Vrueh, R.L., van Veghel, R., Tivel, K.L., Biessen, E.A., Bennett, C.F., Cook, P.D., and van Berkel, T.J. (1997). J. In vivo fate of phosphorothioate antisense oligodeoxynucleotides: predominant uptake by scavenger receptors on endothelial liver cells. Nucleic Acids Res. 25, 3290–3296.

43. Patel, P.C., Giljohann, D.A., Daniel, W.L., Zheng, D., Prigodich, A.E., and Mirkin, C.A. (2010). Scavenger receptors mediate cellular uptake of polyvalent oligonucleotide-functionalized gold nanoparticles. Bioconjugate Chem. 21, 2250–2256.

44. Coles, A.H., Osborn, M.F., Alterman, J.F., Turanov, A.A., Godinho, B.M.D.C., Kennington, L., Chase, K., Aronin, N., and Khvorova, A. (2016). A High-Throughput Method for Direct Detection of Therapeutic Oligonucleotide-Induced Gene Silencing In Vivo. Nucleic Acid Therapeut. 26, 86–92.